International Journal of Development Mathematics Vol 2 Issue 3 Page No. 315 - 331

INTERNATIONAL JOURNAL OF DEVELOPMENT MATHEMATICS

ISSN: 3026-8656 (Print) | 3026-8699 (Online)

Journal homepage: https://ijdm.org.ng/index.php/Journals

Effect of Heat Absorption on Jeffery Fluid Flow in a Saturated Porous Medium with Injection

Nazir Saad[a,b*], Emmanuel Omokhuale[b], Laminu Idris[b] and Samaila Musa[c]

[a]Department of Mathematics, Zamfara State University Talata Mafara, Nigeria.

[b]Department of Mathematical Sciences, Federal University Gusau, Zamfara State, Nigeria.

[c]Department of Computer Science, Federal University Gusau, Zamfara State, Nigeria.

ARTICLE INFO

Article history:
Received 10 July 2025
Received in revised form 20 September 2025
Accepted 24 September 2025

Keywords:
Heat absorption, Jeffery fluid, porous medium, and injection.

MSC 2020 Subject classification:
76S05, 35Q35, 80A20, 76A05

ABSTRACT

The aim of the present paper is to investigate the effect of heat absorption on Jeffery fluid flow in a saturated porous Medium with injection. The coupled nonlinear partial differential equations (PDEs) governing the flow are transformed into ordinary differential equations (ODEs) using regular perturbation technique and solutions for the velocity, temperature and concentration are obtained, also, skin friction, rate of heat and mass transfer was gotten. Computations were carried out to examine the effects of flow parameters such as: Jeffery, heat absorption, magnetic field parameters, Prandtl number, thermal and mass Grashof number and Schmidt number which were graphically depicted and explained. The derived results have been validated with published researches. The research shows that an increase in the Jeffery parameter, heat absorption improve the velocity profiles. Also, both the thermal and mass Grashof numbers enhance the velocity profile, indicating the influence of buoyancy forces driven by temperature and concentration gradients. On the other hand, a similar trend is observed for increasing values of velocity slip and porosity parameters while a reverse pattern is seen for higher magnetic parameter.

1. Introduction

Fluids are partitioned as Newtonian and non-Newtonian fluids. Non-Newtonian fluids have numerous practical and industrial applications, and such fluids involve honey, blood, greases and oils. Polymer industries, textile, irrigation problems and biological systems incorporate flows of non-Newtonian fluids in porous medium encountering magnetic effects. Fluid flow behavior, particularly for non-Newtonian fluids like Jeffrey fluid, over stretching/shrinking sheets embedded in porous media, has significant applications in industrial processes such as polymer extrusion, coating flows, and geothermal energy extraction. Despite extensive research in this area, several unresolved issues persist, particularly in understanding the dual nature of solutions and their stability under varying physical conditions. Several industrial fluids, namely dye, shampoo, adhesives, blood, slurries, food materials, printing inks, cleansers, and dissolved polymers, are non-Newtonian in their physical state (Nagaraju *et al.*, 2024). The application of Jeffrey fluid flow models spans a wide range of industries where accurate prediction and control of non-Newtonian fluid

* Corresponding author. Tel.: +23470959745
E-mail address: nazykaura01@gmail.com **(Nazir Saad)**

https://doi.org/10.62054/ijdm/0203.21

behavior are essential. These models help in optimizing processes, improving product quality, and enhancing the efficiency of various industrial applications. The stated fluids have viscous and viscoelastic properties and are fundamentally nonlinear. The integral equations for aforementioned fluids are naturally more advanced than those for typical Newtonian (Navier-Stokes) fluids (Nagaraju *et al*., 2024).

The study of heat generation or absorption on fluid flow is extremely fundamental in several technological and physical problems of exothermic or endothermic fluid response nowadays, and these effects are crucial in monitoring the heat transference (Gambo *et al.*, 2021). Several scholars have investigated the effects of heat-generating/absorbing fluid on various flow regimes. Effects of heat generation/absorption on free convection MHD flow has considerable importance for many scientific and engineering applications (Omokhuale *et al*., 2016). Razman *et al*. (2022) researched on heat generation. The Jeffrey model can be used in non-Newtonian fluids to explain the stress relaxation property and it produces better approximations to most physiological fluids (Kahshan et al. 2019). Some researchers that conducted researched on the Jeffery fluid are (Akbar *et al*., 2013; Ahmad *et al*., 2024).

Jeffery fluid flow problems are useful in nuclear engineering in connection with the cooling of reactors, in the case of flow past a semi-finite vertical plate under the action of transverses magnetic field and in the presence of suction as reported by Raju *et al*. (2019). It is perceived that a single differential equation is described in the models of Newtonian fluid flows, but in the case of non-Newtonian fluid models, it is not so easy to describe the flow of the model with one and only constitutive differential equation. Usually, the rheological properties of fluids are specified with the help of their hypothetical constitutive conditions. The effects of Hall and ion slip on the radiative magnetohydrodynamic (MHD) rotating flow of viscous incompressible electrically conducting Jeffrey fluid over an infinite vertical flat porous surface by the ramped wall velocity and temperature, and isothermal plate have been explored by Krishna (2022). Krishna (2022) extended and researched on chemical reaction, heat absorption and Newtonian heating on MHD free convective flow. Goud (2020) examined heat generation/absorption influence on steady stretched permeable surface on MHD flow of a micropolar fluid in the presence of variable suction/injection.

Yale *et al*. (2019) studied unsteady heat transfer to MHD oscillatory flow of Jeffrey fluid in a channel filled with porous material. Suction/injection method was first introduced as one of the means for preventing or delaying boundary layer separation. Suction/injection is one of the methods of boundary layer control, which have the aim of reducing losses of energy in channels. Injection is defined as the administering a fluid in to a system as in the case of blood transfusion while in the case of suction is defined as the exclusion of fluid from a system. If the two runs at the same time, then the opposite sides of the plates are porous which

allow the fluid to move in and out. Suction/injection of fluid channels has gained a special concerned due to its paramount applications of different field such as Science, engineering, petroleum drilling industries and food processing industries etc. (Usman *et al*., 2023). Porous media has garnered significant attention in heat transfer, and it removes heat from reactors, heat exchangers, solar energy, etc. Over the past two decades, numerous researchers have dedicated their efforts to studying heat transfer phenomena specifically within porous media. A porous medium is a substance that contains pores, or spaces between solid materials through which liquid or gas can pass. Omowaye *et al*. (2022) presented an analytical method of solution to steady two-dimensional hydromagnetic flow of a viscous incompressible, electrically conducting fluid past a semi-infinite moving permeable plate embedded in a porous medium. It is assumed that the fluid properties are constant except for the fluid viscosity which vary as an inverse linear function of temperature. The boundary layer equations were transformed in to a coupled ordinary differential equation with the help of similarity transformations. They solved the resulting coupled ordinary differential equations were solved using the Homotopy Method (HAM). The combined effect of heat and mass transfer in Jeffrey fluid flow through porous medium over a stretching sheet subject to transverse magnetic field in the presence of heat source/sink was studied by Jena *et al*. (2017). Noor *et al*. (2020) presented a numerical study for the magnetohydrodynamic (MHD) squeezing flow of Jeffrey fluid between two parallel plates in a porous medium with the presence of thermal radiation, heat generation/absorption and chemical reaction. Omokhuale and Dange (2023a) extended this phenomenon to reveal the impact of heat absorption on unsteady MHD convective Jeffery flow of a viscous, electrically conducting and incompressible fluid. Furthermore, Omokhuale and Dange (2023b) focused on extending their research to investigate chemical reaction and radiation absorption effects on MHD Jeffery fluid. Disu *et al.* (2024) investigated the impact of species absorption of Jeffery fluid flow through a saturated permeable medium with variable thermal conductivity. The dimensional partial nonlinear derivative model controlling the chemical reacting fluid flow is transformed to invariant form. The resulting flow equations in their work are computed numerically using an approximated finite implicit Crack-Nicolson.

Recently, Krishna *et al*. (2025) studied thermal radiation and rotational effects on MHD free convection flow of Jeffreys fluid past an infinite, perpendicular, absorbent plate has significant applications in various fields due to the complex interactions among fluid dynamics, heat transfer, magnetic fields, and the unique properties of Jeffreys fluid. Naz and Tamizharasi (2025) examined the effects of varying transient magnetic fields and their orientations on boundary layers aids in understanding the flow in complex surface geometries, turbulence control, drag reduction, aircraft and ship design, groundwater management, and the

study of construction and coastal engineering. The study introduces a novel dynamic of the boundary layer of a natural convective Jeffrey fluid flowing over an erect porous moving plate.

The main objective of this paper was to examine analytically the effect of heat absorption on Jeffery fluid flow in a saturated porous medium considering injection. The governing equations are solved employing regular perturbation technique to derive solutions for the velocity, temperature and concentration. Skin-friction, rate of heat and mass transfer were also obtained. The effects of physical parameters of interest on the velocity, temperature and concentration profiles were depicted graphically and discussed.

2. Mathematical Formulation

Consider the flow of incompressible Jeffery fluid in a vertical plate with saturated porous medium chosen along the plate under the influence of an externally applied homogeneous magnetic field. A magnetic field of uniform strength B_0 is applied transversely to the plate. The flow is further assumed to be in the $x' -$ axis direction which is taken to be vertically upward along the channel walls and $y' -$ axis is taken to be normal to the plate that are ∞ distance apart. Initially, the plate and the fluid are at same temperature T' with concentration level C' at time $t' > 0$, the plate and the mass concentration are raised to T'_w and C'_w causing the presence of temperature and concentration difference to be $T' - T'_\infty$ and $C' - C'_\infty$, respectively. The effects of injection and heat absorption are considered. Following Omokhuale and Dange (2023a), The study of heat generation or absorption on fluid flow is extremely fundamental in several technological and physical problems of exothermic or endothermic fluid response nowadays, and these effects are crucial in monitoring the heat transference (Gambo *et al*., 2021). Several scholars have investigated the effects of heat-generating/absorbing fluid on various flow regimes. and under the usual Boussinesq's approximation, the governing equations in dimensional form are continuity, momentum, energy and mass equations which are as follows:

$$\frac{\partial v}{\partial y} = 0 \tag{1}$$

$$\frac{\partial U'}{\partial t^I} + v'\frac{\partial U'}{\partial y^I} = \frac{\upsilon}{I+\lambda}\frac{\partial^2 U'}{\partial y^{1^2}} + g\beta_T\left(T' - T'_\infty\right) + g\beta_C(c' - C'_\infty) - \nu\frac{U'}{K'} - \frac{\sigma B_0^2}{\rho}U' \tag{2}$$

$$\frac{\partial T'}{\partial t'} + v'\frac{\partial T'}{\partial y'} = \frac{K_T}{\rho cp}\frac{\partial^2 T'}{\partial y^{I2}} + \frac{\theta'}{\rho cp}\left(T' - T'_\infty\right) + \theta'_1\left(C' - C'_\infty\right) \tag{3}$$

$$\frac{\partial C'}{\partial t^I} + v'\frac{\partial C'}{\partial y^I} = D'\frac{\partial^2 C'}{\partial y^{1^2}} - R'_c(C' - C'_\infty) \tag{4}$$

Subject to the initial and boundary conditions:

$$t' \le 0: u' = 0, T' = T'_\infty, C' = C'_\infty \text{ for all } y'$$

$$t' > 0\begin{cases} u' = \varphi\frac{du'}{dy'}T' = T'_\infty + (T'_w - T'_\infty)\epsilon e^{iwt}, C' = C'_\infty + (C'_w - C'_\infty)\epsilon e^{iwt} at\ y' = 0 \\ u' \to 0, T' \to T^I_\infty, C' \to C^I_\infty \quad as\ y' \to \infty \end{cases} \tag{5}$$

Here, $v' = + v_0$ (6)

We define the following dimensionless quantities:

$$y = \frac{y^1 U_o}{\nu}, t = \frac{t^1 U_o^2}{\upsilon}, U = \frac{u^I}{u_o}, \theta = \frac{T^I - T^I_\infty}{T^I_w - T^I_\infty}, \xi = \frac{C^I - C^I_\infty}{C^I_w - C^I_\infty} \tag{7}$$

Substituting (6) and (7) into equations (2), (3) and (4), then, we have the following non – dimensional form of these equations as follows:

$$\frac{\partial u}{\partial t}+\beta\frac{\partial u}{\partial y}=\frac{I}{I+\lambda_1}\frac{\partial^2 U}{\partial y^2}+G_1\xi+G_2\,\theta-\frac{I}{K}u-Mu \tag{8}$$

$$\frac{\partial \theta}{\partial t}+\beta\frac{\partial \theta}{\partial y}=\frac{I}{Pr}\frac{\partial^2 \theta}{\partial y^2}+\phi\theta+\delta\xi \tag{9}$$

$$\frac{\partial \xi}{\partial t}+\beta\frac{\partial \xi}{\partial y}=\frac{I}{Sc}\frac{\partial^2 \xi}{\partial y^2}-\gamma\xi \tag{10}$$

The corresponding initial and boundary conditions (5) in non-dimensional form become:

$$\begin{cases} u=u-\varphi\frac{du}{dy}\quad \theta=1+\epsilon e^{iwt},\xi=1+\epsilon e^{iwt},\mathrm{y}=0 \\ u\to 0,\theta\to 0,\xi\to 0\quad as\ y\to\infty \end{cases} \tag{11}$$

where $=\frac{U_0}{U_0}$, M=$\frac{\delta\beta_0^2}{U_0^2}$, K=$\frac{K'U_0}{\nu^2}$, G1=$\frac{GB_T(T_W'-T_\infty')\nu\xi}{U_0^3}$, G1=$\frac{GB_T(C_W'-C_\infty')\nu\xi}{U_0^3}$.

3. Analytical Solutions

To solve (8) to (10) subject to the boundary conditions (11), we assume approximate solutions of the form:

$u(y,t)=u_o\,(\mathrm{y})+u_1(\mathrm{y})\epsilon e^{int}$ (12)

$\xi(\mathrm{y,t})=\xi_o(\mathrm{y})+\xi_1(\mathrm{y})\epsilon e^{int}$ (13)

$\theta(\mathrm{y\ t})=\theta_o(\mathrm{y})+\theta_1(\mathrm{y})\epsilon e^{int}$ (14)

Substituting (12) to (14) into (8) to (11), we have

The following are set of ODEs:

$\theta_o:\theta_o''+\beta pr\theta_o'+\beta pr\theta_o=-\lambda pr\xi_o$ (15)

$\theta_1:\phi_1''-\beta pr\theta_I'+(\gamma+in)pr\,\theta_1=-\lambda pr\xi_1$ (16)

$\xi_o:\xi_o''-\beta sc\,\xi_o'+ksc\xi_o=0$ (17)

$\xi_1:\xi_I''+\beta sc\,\xi_I'-(k+in)pr\xi_I=0$ (18)

$u_o:\frac{1}{1+\lambda}u_0''-\beta\,u_0'-(\mathrm{M}+\frac{1}{K})\,u_0=-G_1\,\xi_0-G_2\theta_0$ (19)

$u_1:\frac{1}{1+\lambda}u_0''-\beta\,u_1'-(M+\frac{1}{K}+in)u_1=-G_1\xi_1-G_2\theta_1$ (20)

The corresponding boundary conditions are:

$u_o-\varphi u_0'=0$, $u_o=\varphi u_0'$, $\theta_0=1$, $\theta_1=1$, $\xi_0=1$, $\xi_1=1$ at y=0

$u_0=u_1=0\qquad \theta_0=\theta_1=0\qquad \xi_0=\xi_1=0\qquad$ as $y\to\infty$ (21)

Solving equations (16) to (20) subject to the following boundary condition (21):

The approximate solutions of velocity, temperature and concentration are expressed in the following form, respectively:

$u(y,t)=W_{12}\,e^{-f_{10}\mathrm{y}}+W_{13}\,e^{-f_2\mathrm{y}}+W_{14}\,e^{-f_6\mathrm{y}}+W_{15}\,e^{-f_2\mathrm{y}}+(W_{17}\,e^{-f_{12}\mathrm{y}}+W_{18}\,e^{-f_4\mathrm{y}}+W_{19}\,e^{-f_8\mathrm{y}}+W_{20}\,e^{-f_4\mathrm{y}})\,\varepsilon e^{int}$ (22)

$\theta(\mathrm{y,t})=W_6\,e^{-f_6\mathrm{y}}+W_7\,e^{-f_6\mathrm{y}}+(W_9\,e^{-f_8\mathrm{y}}+W_{10}\,e^{-f_4\mathrm{y}})\,\varepsilon e^{int}$ (23)

$\xi(\mathrm{y,t})=e^{-f_2 y}+e^{-f_4 y}\,\varepsilon e^{int}$ (24)

The Skin-friction, Nusselt and Sherwood numbers respectively at surface are as follows:

$\lfloor u\,(0)\rfloor=-f_2\,W_{12}-f_6W_{14}-f_2W_{15}-(f_{11}\,w_{12}+f_2w_{13}+f_6w_{14}+f_2w_{15})\,\varepsilon e^{int}$ (25)

$$\lfloor u\,(1)\rfloor = -\,f_4\,w_{18} - f_{8w_{19}} - f_{4w_{20}} - (f_{12}\,w_{17} + f_4 w_{18} + f_8 w_{19} + f_4 w_{20})\varepsilon e^{int} \quad (26)$$

$$\lfloor \theta\,(0)\rfloor = -f_2 - (f_4)\,\varepsilon e^{int} \quad (27)$$

$$\lfloor \theta\,(1)\rfloor = -F_2 e^{-F_4} - (F_4 e^{-F_8})\,\varepsilon e^{int} \quad (28)$$

$$\lfloor \xi\,(0)\rfloor = -F_6 - (-f_2 -)\,(f_{12})\,\varepsilon e^{int} \quad (29)$$

$$\lfloor \xi\,(1)\rfloor = -F_6 e^{-F_6} - (f_2\,e^{-F_2} -)\,(f_{12})\,\varepsilon e^{int} \quad (30)$$

3. Result and Discussion

The effect heat absorption on Jeffery fluid saturated in a porous medium with injection has been formulated and solved analytically by regular perturbation technique. In order to understand the flow of the fluid computations are performed for different parameters such as: G1, G2, Sc, Pr, M, K, λ, γ and β.

3.1 Velocity Profiles

Figures 1 and 2 display the velocity profiles for different thermal Grashof number ($G1$) and Mass Grashof number ($G2$). The Grashof number for heat transfer signifies the relative effect of the thermal buoyancy force to the viscous hydrodynamic force in the boundary layer. As expected, it is observed that there is an enhancement in the velocity due to the rising of thermal buoyancy force. Also, as G1 increases, the peak values of the velocity increases rapidly near the porous plate and then decays smoothly to the free stream velocity. The modified Grashof number defines the ratio of the species buoyancy force to the viscous hydrodynamic force. As expected, the fluid velocity increases and the peak value is more distinctive due to increase in the species buoyancy force. The velocity distribution attains a distinctive maximum value in the vicinity of the plate and then decreases properly to approach the free stream value. It is noticed that the velocity increases with increasing values of the Grashof number for mass transfer. In the case of different values of Magnetic parameter, the profiles of the velocity of the boundary layer is presented in Figure 3. The velocity decreases with an increase in the Hartmann number. It is because that the application of transverse magnetic field will result a resistive type force (Lorentz force) similar to drag force which tends to resist the fluid flow and thus reducing its velocity. Also, the boundary layer thickness decreases with an increase in the Hartmann number. Figure 4 presents the velocity profile for different values of Permeability parameter (K). It is found that as K rises the velocity of the fluid increases. In the boundary layer, the velocity starts by increasing to a maximum, and slowly decreases. Physically, Permeability parameter indicates thermal buoyancy characteristic of a fluid flow. The greater it gets, the more the buoyant force brought about by the temperature gradient acts upon the fluid, thereby increasing its velocity rate in the vicinity of the heated surface. The peak velocity occurs in the boundary layer where the forces of buoyancy prevail over that of viscosity. Figure 5 depicts the velocity profiles for different values of heat absorption parameter (γ). The momentum boundary layer decreases when the intensity of the heat absorption increases. The effect of slip parameter (ψ) on the velocity profile is graphically presented in Figure 6. The velocity increases as the velocity slip effect becomes significant. Figure 7 illustrates the effect of injection parameter (β) on the velocity profiles. It is observed that the velocity increases as β becomes significant. The effect of heat absorption parameter (ϕ) on the velocity profile is presented in Figure 8. It is evident that the momentum boundary layer becomes higher as (ϕ) is increased. The

velocity profiles of Figure 9 demonstrate the velocity profiles for different values of mass absorption parameter ( ). It is found that the velocity rises with increase in δ. Figure 10 displays the velocity profiles for different values of (S_c). It is noticed that the velocity increases as s_c rises. In Figure 11, the effect of Prandtl number on the velocity profiles is shown. It is clear that the velocity boundary layer increases when the Prandtl number is increased. Figure 12 connotes the velocity profile for varied values of Jeffery parameter $(\lambda 1)$. It is seen that higher value of Jeffery parameter leads to rise in the velocity of the fluid.

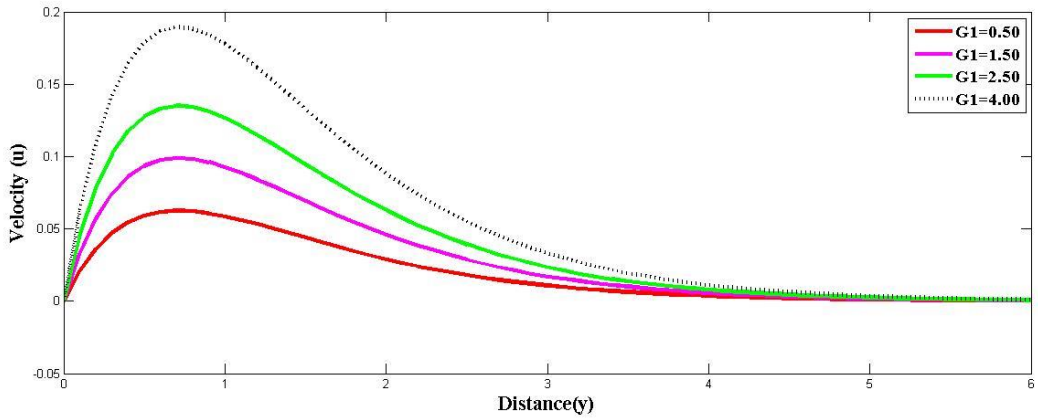

Figure 1: Velocity profile for different values of G1.

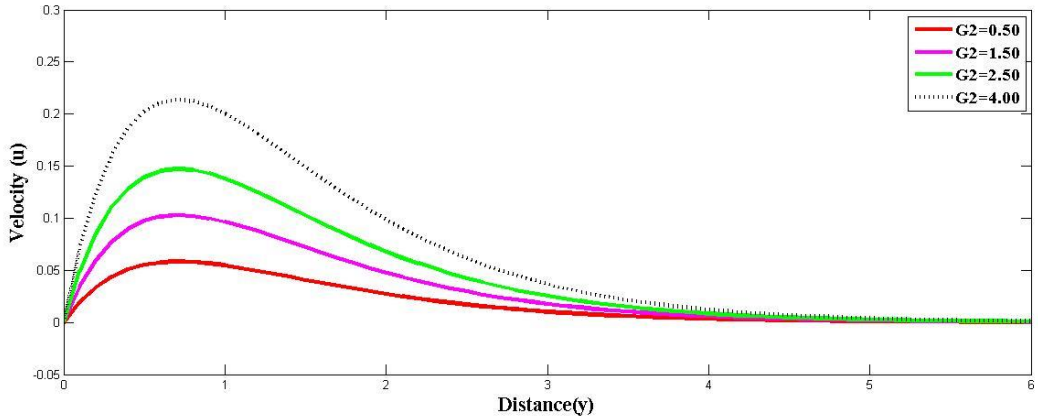

Figure 2: Velocity profile for different values of G2.

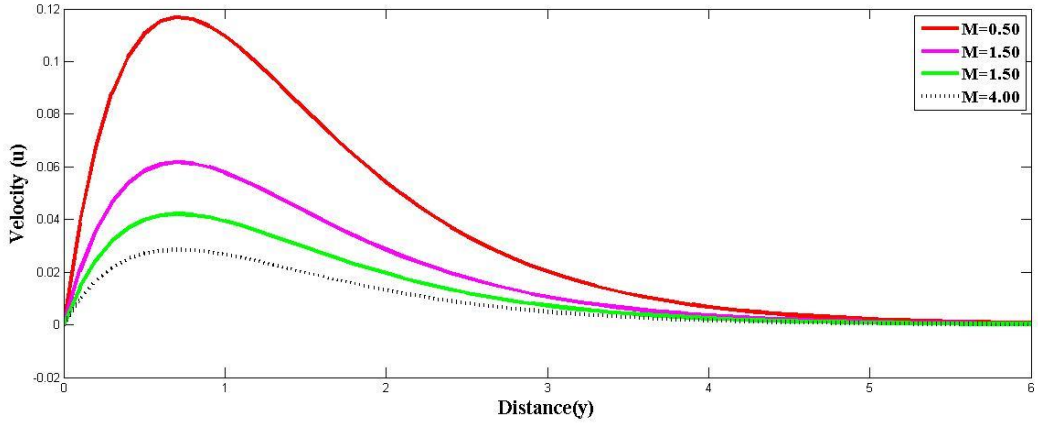

Figure 3: Velocity profile for different values of M

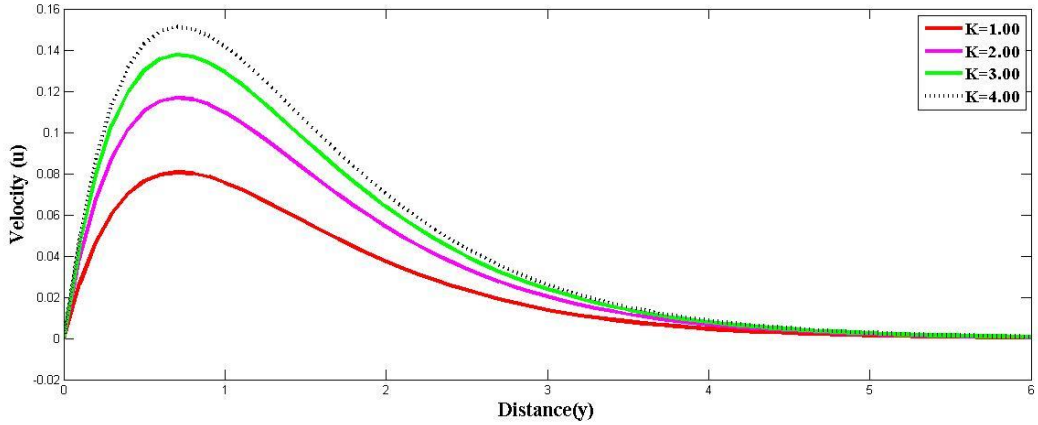

Figure 4: Velocity profile for different values of K.

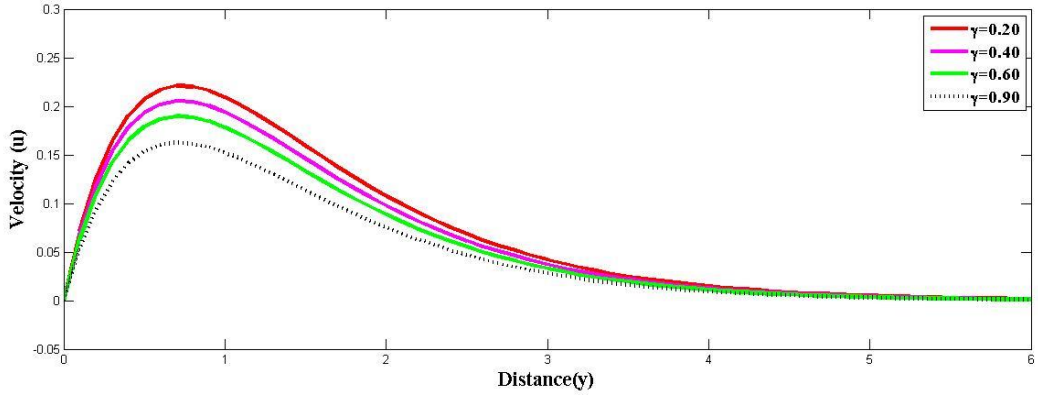

Figure5 : Velocity profile for different values of γ.

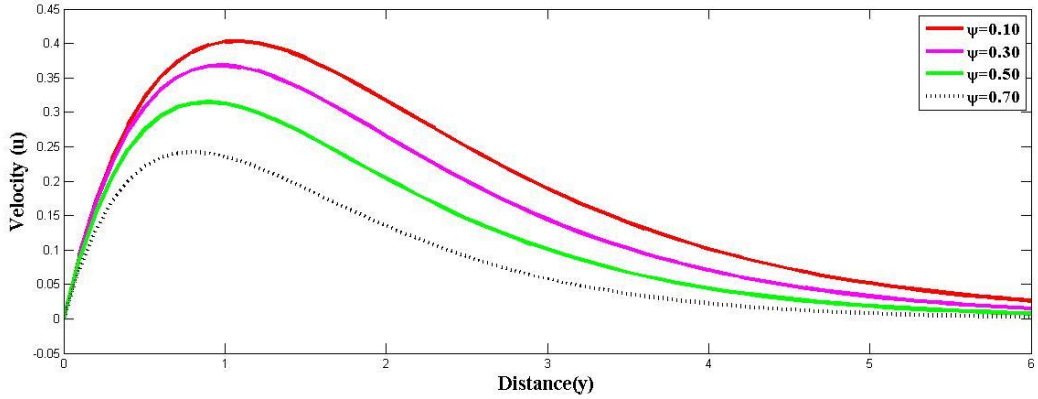

Figure 6: Velocity profile for different values of φ.

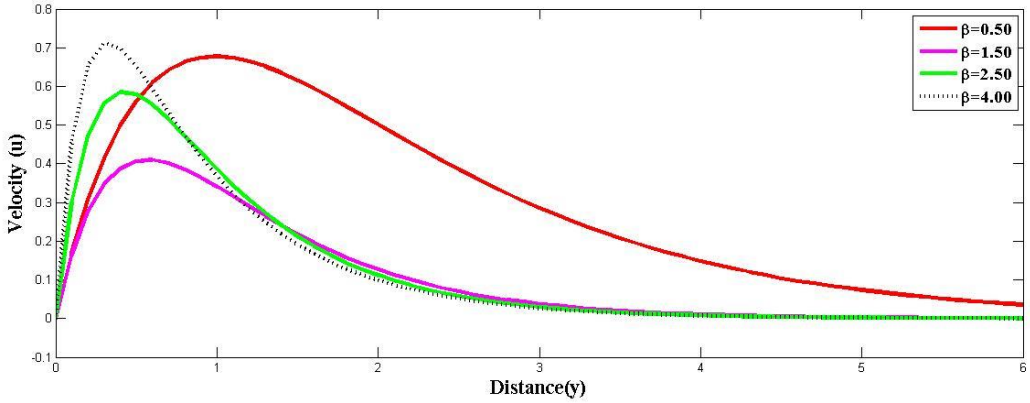

Figure 7: Velocity profile for different values of β.

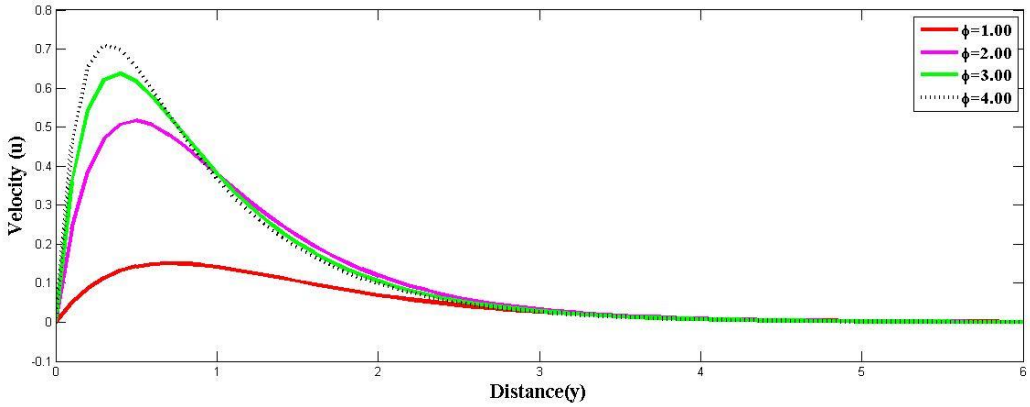

Figure 8: Velocity profile for different values of ϕ.

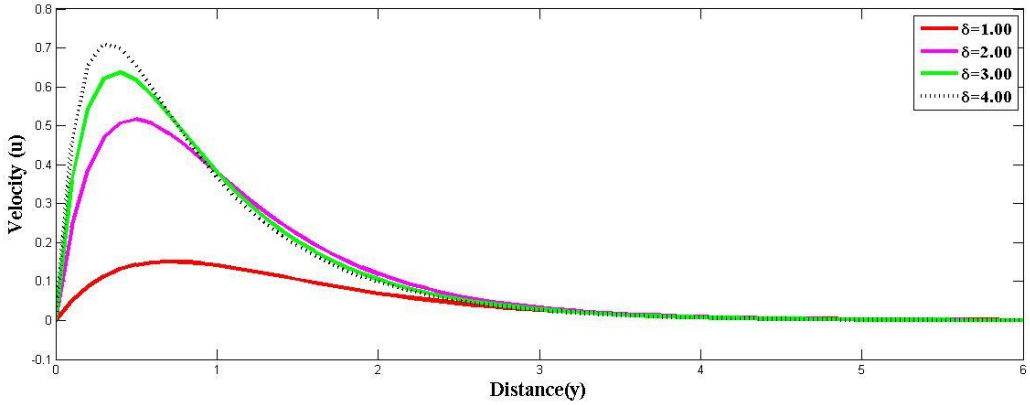

Figure 9: Velocity profile for different values of δ.

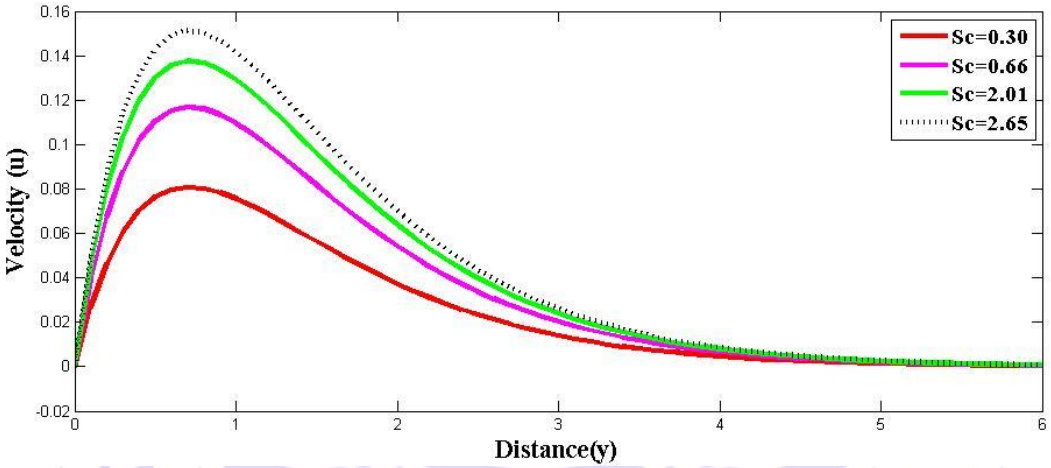

Figure 10: Velocity profile for different values of Sc.

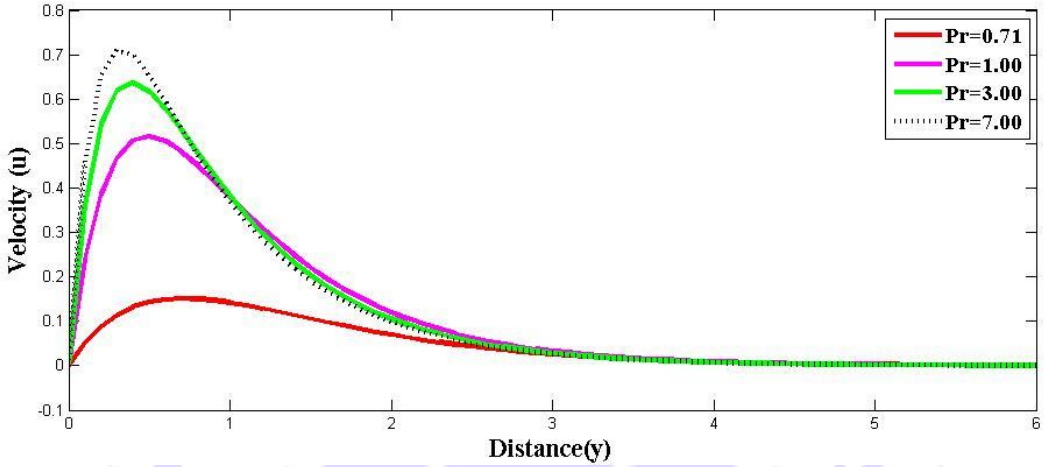

Figure 11: Velocity profile for different values of Pr.

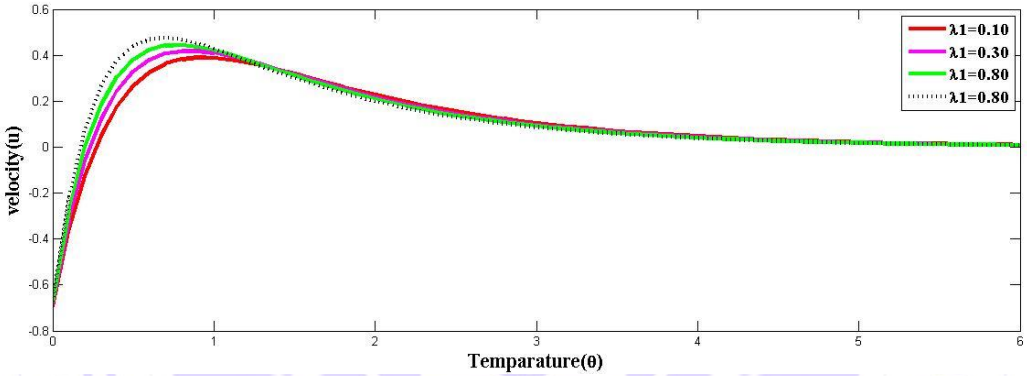

Figure 12: Velocity profile for different values of$\lambda 1$.

3.2 Temperature profile

Figure 13 represents the impact of Prandtl number Pr on the temperature profiles. It is found that increase in Prandtl number causes a decrease in the thermal boundary layer of the fluid, because, either increases of kinematic viscosity or decrease of thermal conductivity leads to increase in the value of Prandtl number. Hence temperature decreases with increasing of Prandtl number. The effect of the mass absorption parameter on the temperature field is displayed in Figure 14. It is depicted that the temperature of the fluid rises as mass absorption becomes significant. Figure 15 displays velocity profiles for different values of heat absorption parameter (ϕ). It is obvious that as ϕ increases the thermal boundary layer rises. Figure 16 exhibits the effect of injection parameter on the temperature of the fluid. It is shown that as injection rises the temperature within the boundary layer is higher.

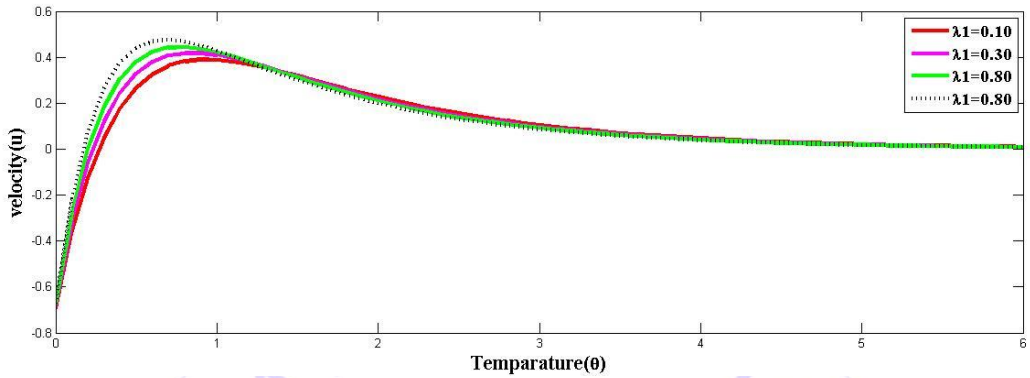

Figure 13: Temperature profile for different values of Pr.

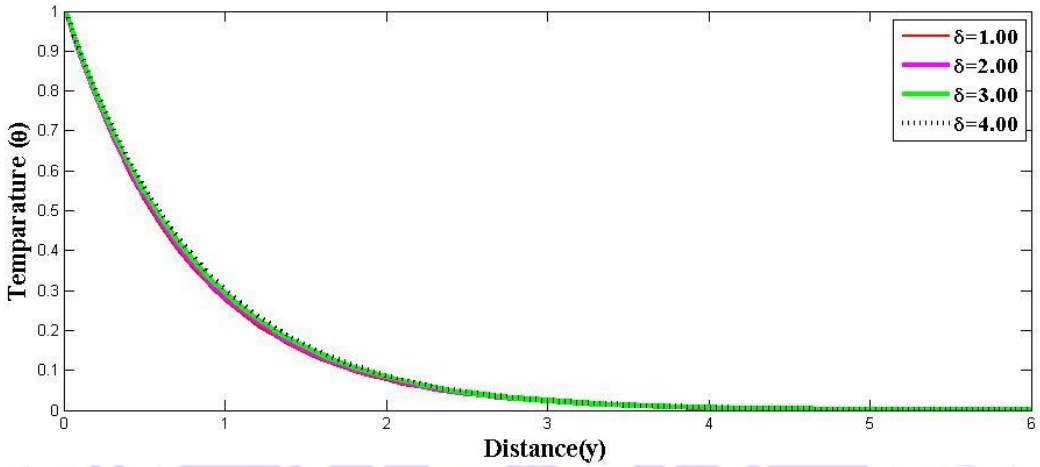

Figure 14: Temperature profile for different values of δ

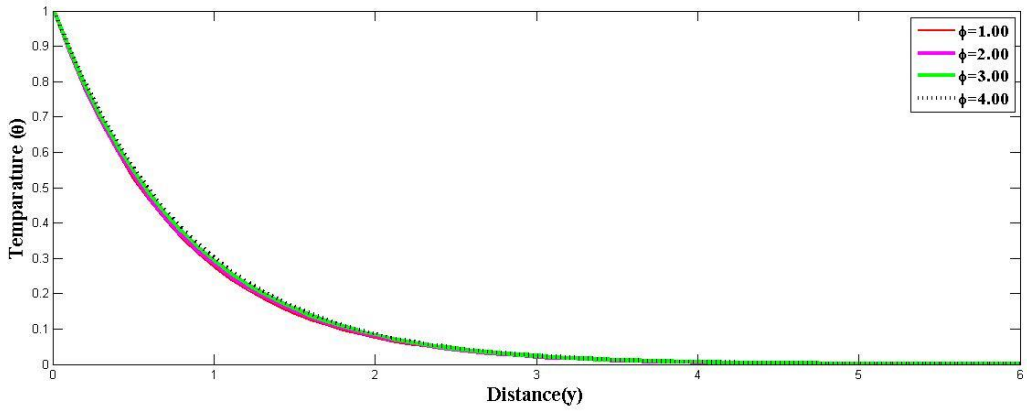

Figure 15: Temperature profile for different values of φ.

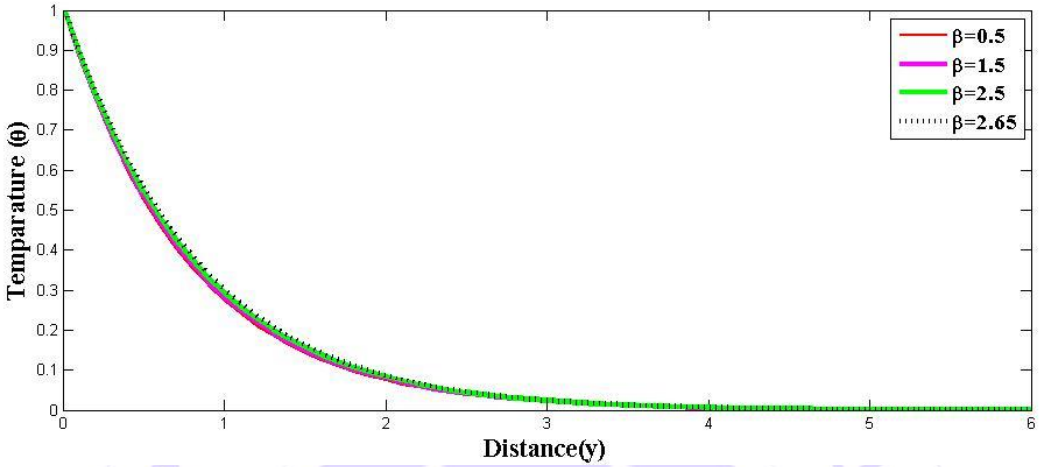

Figure 16: Temperature profile for different values of β.

3.3 Concentration profiles

Figure 17 depicts the effect of chemical reaction parameter on the concentration profiles. It is seen that the concentration of the fluid becomes lower as chemical reaction becomes significant. The concentration profiles of Figure 18 demonstrate the concentration profiles for varied Schmidt numbers. It is noticed that the concentration decreases with increase in Schmidt value (Sc). The causes a narrower concentration boundary layer and reduced penetration of a solute in the fluid. Because the steeper concentration gradients are associated with slower diffusion of mass with increasing Sc. This causes a narrower concentration boundary layer and reduced penetration of a solute in the fluid, because, Schmidt number is a dimensionless number defined as the ratio of momentum diffusivity and mass diffusivity, and is used to characterize fluid flows in which there are simultaneous momentum and mass diffusion convection processes. Therefore, concentration boundary layer decreases with an increase in Schmidt number. Figure 19 shows the plot of the concentration profiles for different values of injection parameter. It is seen that the mass boundary layer decreases as β is increased.

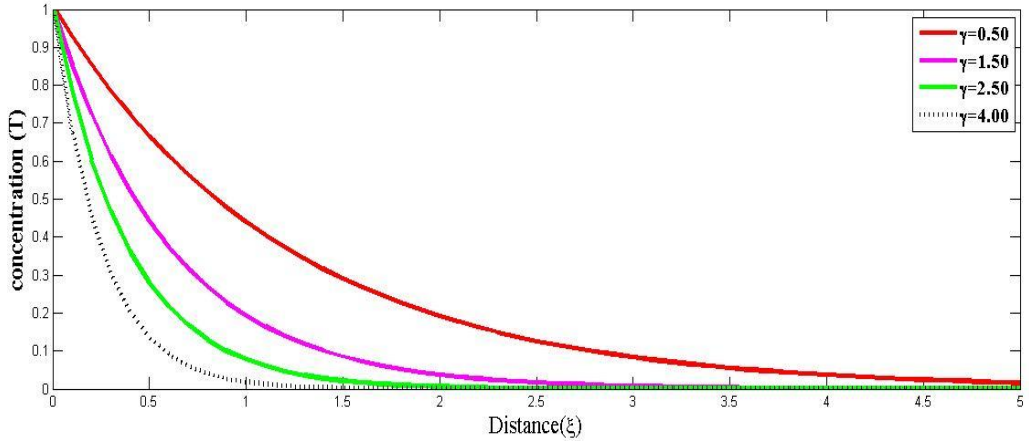

Figure 17: Concentration profile for different values of γ

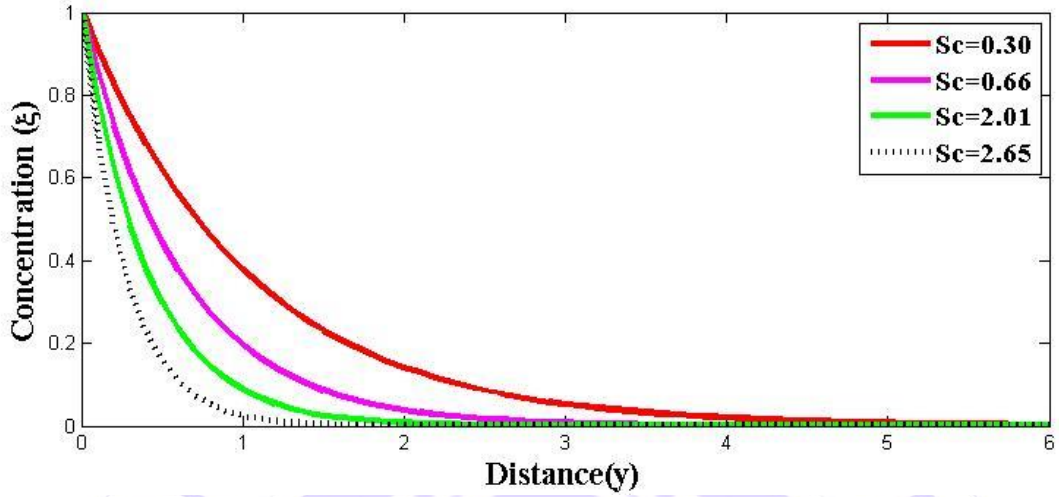

Figure 18: Concentration profile for different values of Sc

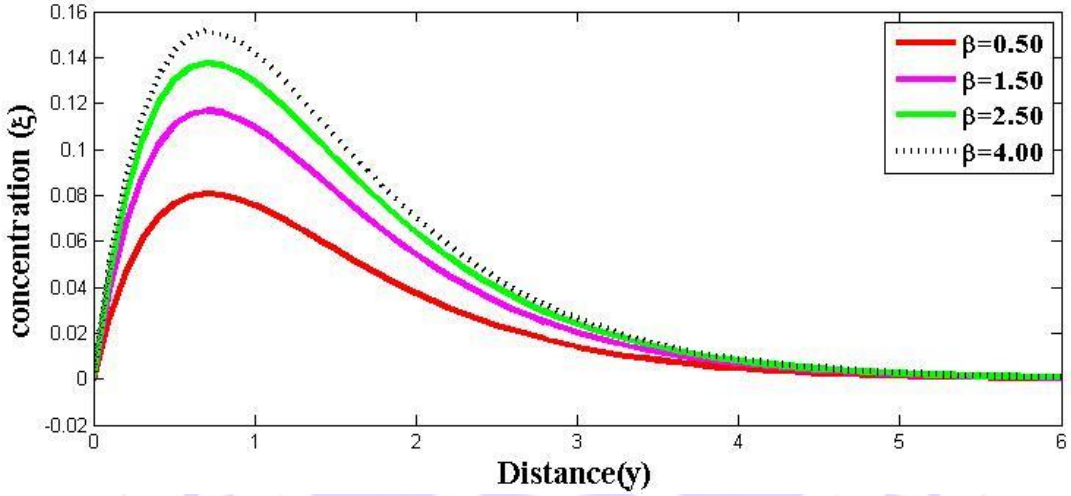

Figure 19: Concentration profile for different values of β

4. Conclusion

The current paper gives the analytical solution of velocity slip effect of heat absorption on Jeffery fluid flow in a saturated porous medium in the presence of injection and chemical reaction mechanisms. Specifically, the governing boundary layer equations are made up with suitable boundary conditions. The boundary layer equations are simplified and non-dimensionalized. The velocity, temperature and concentration solutions are obtained by regular perturbation method. The effects of the relevant parameters on the velocity, temperature and concentration profiles are shown graphically. Our results are compared with the research conducted by Omokhuale and Dange (2023a), and a very good agreement is found. The most significant conclusion are as follows:

1. An increase in the Jeffery parameter, heat absorption improve the velocity profiles.

2. Both the thermal and mass Grashof numbers enhance the velocity profile, indicating the influence of buoyancy forces driven by temperature and concentration gradients. On the other hand, a similar trend is observed for increasing values of velocity slip and porosity parameters while a reverse pattern is seen for higher magnetic parameter.
3. Both Schmidt and Prandtl numbers lead to a fall in the momentum, mass and thermal boundary layers. An opposite trend is found as injection become significant.

The concentration of the fluid reduces as chemical reaction parameter rises while increase in mass absorption parameter causes an increase in the fluid's velocity and temperature.

References

Ahmad, S. K., Muhammad, H. A., Hamza, M. M., Ojemeri, G. and Usman, U. (2024). Magnetized Oscillatory Jeffrey Fluid Flow in A Porous Channel with Unequal Wall Temperature, *Dutse Journal of Pure and Applied Sciences (DUJOPAS)*, 10(2c), 261-272. https://doi.org/10.4314/dujopas.v10i2c.240

Akbar, N. S., Nadeem, S. and Lee, C. (2013). Characteristics of Jeffrey fluid model for peristaltic flow of chyme in small intestine with magnetic field, *Results in Physics*, 3, pp. 152–160.

Disu, A. B., Omokhuale, E., & Salawu, S. O. (2024). Effect of chemical absorption on Jeffery Fluid Flow in saturated Porous Media with variable thermal conductivity. *Journal of Natural Sciences and Mathematics Research*, *10*(1), 93-105.

Gambo D., Yusuf, T. S., Oluwagbemiga, S. A., Kozah, J. D. and Gambo J. J. (2021). Analysis of free convective hydromagnetic flow of heat generating/absorbing fluid in an annulus with isothermal and adiabatic boundaries. Partial Differential Equations in Applied Mathematics. https://doi.org/10.1016/j.padiff.2021.100080

Goud, B. S. (2020). Heat generation/absorption influence on steady stretched permeable surface on MHD flow of a micropolar fluid through a porous medium in the presence of variable suction/injection. *International Journal of Thermofluids*, *7*, 100044.

Jena, S., Mishra, S. R., & Dash, G. C. (2017). Chemical reaction effect on MHD Jeffery fluid flow over a stretching sheet through porous media with heat generation/absorption. *International Journal of Applied and Computational Mathematics*, *3*(2), 1225-1238. https://doi.org/10.1007/s40819-016-0173-8

Kahshan, M., Lu, D. and Siddiqui, A. M. (2019). A Jeffrey Fluid Model for a Porous-walled Channel: Application to Flat Plate Dialyzer, *Scientific Reports*, 9. pp. 15-25

Krishna, M. V. (2022). Chemical reaction, heat absorption and Newtonian heating on MHD free

convective Casson hybrid nanofluids past an infinite oscillating vertical porous plate. *International Communications in Heat and Mass Transfer*, *138*. doi.org/10.1016/j.icheatmasstransfer.2022.106327

Krishna, M. V., Gopal, C. H., Sudhakar, M., & Rao, S. M. (2025). Radiation and rotation effects on MHD free convection flow of Jeffreys fluid over an infinite vertical absorbent plate. *Multiscale and Multidisciplinary Modeling, Experiments and Design*, *8*(6), 298. https://doi.org/10.1007/s41939-025-00882-4

Nagaraju, B., Kishan, N., Tawade, J. V., Meenapandi, P., Abdullaeva, B., Waqas, M., Gupta, M. Batool, N. & Ahmad, F. (2024). Analysis of boundary layer flow of a Jeffrey fluid over a stretching or shrinking sheet immersed in a porous medium. *Partial Differential Equations in Applied Mathematics*, *12*. https://doi.org/10.1016/j.padiff.2024.100951

Naz, S., & Tamizharasi R. (2025). The Impact of a Non-Uniform and Transient Magnetic Field on Natural Convective Jeffrey Fluid Flowing over a Heated Porous Plate: A Comparitive Study. *Journal of Computational and Theoretical Transport*, *54*(1), 1-21.

Noor, N. A. M., Shafie, S., & Admon, M. A. (2020). Unsteady MHD squeezing flow of Jeffrey fluid in a porous medium with thermal radiation, heat generation/absorption and chemical reaction. *Physica Scripta*, *95*(10). https://doi.org/10.1088/1402-4896/abb695

Omokhuale, E. Usman, H. and Altine, M. M. (2016). Effect of Heat Absorption on Steady/Unsteady MHD Free Convection Heat and Mass Transfer Flow Past an Infinite Vertical Permeable Plate with Mass Absorption and Variable Suction. *Journal of the Nigerian Association of Mathematical Physics,* Volume 38 (Nov., 2016). 433 – 442.

Omokhuale, E., & Dange, M. S. (2023a). Heat absorption effect on magnetohydrodynamic (MHD) flow of Jeffery fluid in an infinite vertical plate. *FUDMA Journal of Sciences*, *7*(2), 45-51. https://doi.org/10.33003/fjs-2023-0702-1200

Omokhuale, E., & Dange, M. S. (2023b). Radiation Absorption and Chemical Reaction Effects on Magnetohydrodynamic (MHD) Flow of Jeffery Fluid in an Infinite Vertical Plate. In *Journal of Pure and Applied Sciences (Science Forum,* 23(1), 417-428.

Omowaye, A.J. Fagbade, A.I. Ajayi, A.O. (2015). Dufour and Soret effects on steady MHD convective flow of a fluid in a porous medium with temperature dependent viscosity: Homotopy analysis approach. *Journal of the Nigerian Mathematical Society*, 34, 343 – 360. https://doi.org/10.1016/j. jnnms.2015.08.001.

Raju, R. S., Reddy, G. J., Kumar, M. A., & Gorla, R. S. R. (2019). Jeffrey fluid impact on MHD free convective flow past a vertically inclined plate with transfer effects: EFGM solutions. *International Journal of Fluid Mechanics Research*, *46*(3). https://doi:10.1615/InterJFluidMechRes.2018024682

Ramzan, M., Shafique, A. and Nazar, M. (2022). MHD flow of second grade fluid with heat absorption and chemical reaction. *International Journal of theoretical and Applied Mathematics*, 8(2), 30 – 39. https://doi:10.11648/j.ijtam.20220802.11

Usman, H., Rufa'I, T. U. A., & Omokhuale, E. (2022). Effects of Suction/Injection on Free Convective Radiative Flow In A Vertical Porous Channel With Mass Transfer And Chemical Reaction. *International Journal of Science for Global Sustainability (IJSGS)*, *8*(4). https://doi.org/10.57233/ijsgs.v8i4.364x

Yale, I. D., Aisha, A. H., Ibrahim, M., & Murtala, M. (2019). Unsteady Heat Transfer to MHD Oscillatory Flow of Jeffrey fluid in a Channel Filled with Porous Material. *International Journal of Scientific and Research Publications*, *9*(7), 641-645.

Appendix

$$n_1 = \sqrt{\frac{(-\beta Sc)^2+4(KSc)}{4}},\ n_2 = \sqrt{\frac{(\beta Sc)^2+4(R+in)Sc}{4}}, f_1 = \frac{\beta pr}{2} + n_1,\ f_4 = \frac{-\beta pr}{2} + n_2,$$

$$W_3 = 1, W_7 = \frac{f_2 \lambda pr}{f_2^2 - f_2 + \lambda pr}, W_4 = 1, n_3 = \sqrt{\frac{(\beta pr)^2+4(\gamma pr)}{4}}, n_4 = \sqrt{\frac{(\beta pr)^2+4(\gamma - in)pr}{4}}$$

$$f_5 = \frac{\beta pr}{2} + n_3,\ f_6 = \frac{\beta pr}{2} + n_4, W_6 = 1 - W_7, W_7 = \frac{f_2 \lambda pr}{f_2^2 - f_2 + \lambda pr}, W_9 = 1 - W_{10}$$

$$W_{10} = \frac{\lambda pr}{f_4^2 - f_4 + (\gamma - in)pr},\ n_5 = 1+\lambda,\ n_6 = \sqrt{\frac{(\beta n5)^2+4\left(m+\frac{1}{k}\right)n5}{4}}, n_7 = \sqrt{\frac{(\beta n5)^2+4\left(m+\frac{1}{k}+in\right)n5}{4}}$$

$$f_{10} = \frac{\beta n5}{2} + n_5, f_{12} = \frac{\beta n5}{2} + n_7, W_{12} = \frac{-w_{13}(1+\psi f_2) - w_{14}(1+\psi f_6) - w_{15}(1+\psi f_2)}{(1+\psi f_{10})}$$

$$W_{13} = \frac{-G_1 n5}{f_2^2 - \beta n5 f_2 - \left(m+\frac{1}{k}\right)n5}, W_{14} = \frac{-G_2 n5}{f_2^2 - \beta n5 f_6 - \left(m+\frac{1}{k}\right)n5}, W_{15} = \frac{-G_2 n5}{f_2^2 - \beta n5 f_2 - \left(m+\frac{1}{k}\right)n5}$$

$$W_{17} = \frac{-w_{18}(1+\psi f_4) - w_{19}(1+\psi f_8) - w_{20}(1+\psi f_4)}{(1+\psi f_{12})}, W_{18} = \frac{-G_2 n5}{f_4^2 - \beta n5 f_2 - \left(m+\frac{1}{k}+in\right)n5}$$

$$W_{19} = \frac{-G_2 n5}{f_8^2 - \beta n5 f_8 - \left(m+\frac{1}{k}+in\right)n5}, W_{20} = \frac{-G_2 n5}{f_4^2 - \beta n5 f_4 - \left(m+\frac{1}{k}+in\right)n5}$$